

Nonlinear Local Control of the Safety-Factor-Profile Gradient at Moving Spatial Locations in Tokamak Plasmas*

Sai Tej Paruchuri, Andres Pajares, and Eugenio Schuster

Abstract—Tokamaks are toroidal devices that confine a very hot plasma (hydrogenic ionized gas) by using strong magnetic fields. When the kinetic energy is high, positively charged nuclei in the plasma can overcome the Coulombic forces of repulsion and fuse to form a heavier nucleus. A tremendous amount of energy is released during this reaction. The pitch of the magnetic field in a tokamak, measured by the safety factor profile q , plays a crucial role in ensuring the magnetohydrodynamic (MHD) stability of the tokamak plasma. MHD instabilities like the Neoclassical Tearing Mode (NTM), which can deteriorate or even terminate plasma confinement, can appear at regions in the tokamak where the safety factor profile assumes a rational value. Since the safety factor profile is a continuous function of location in the tokamak, rational values at specific locations are inevitable. Controlling the gradient of the safety factor profile at these locations can prevent or mitigate the effect of MHD instabilities. In this work, a one-dimensional model that approximates the safety factor gradient dynamics at one of the locations where the safety factor q achieves a rational value is developed. A controller based on feedback linearization of this model is designed to track a target gradient value in the steady-state scenario. The effectiveness of this controller is demonstrated in nonlinear numerical simulations powered by the Control Oriented Transport SIMulator (COTSIM) for a DIII-D tokamak scenario.

I. INTRODUCTION

Nuclear fusion is a reaction in which two or more nuclei combine to form larger nuclei and subatomic particles. The difference in mass between reactants and products is released in the form of energy. However, sustained nuclear fusion for energy production is challenging to achieve and is still an active research area. *Tokamaks* are torus-shaped devices that use powerful magnetic fields to confine a plasma (hot ionized gas) consisting of charged ions and electrons. They are considered one of the most promising devices for realizing nuclear fusion. The confined plasma in a tokamak can reach temperatures as high as ten times the temperature of the sun's core. At such high temperatures, the ions in the plasma have sufficient kinetic energy to overcome the Coulombic forces of repulsion and achieve nuclear fusion [1].

The safety factor q , a measure of the pitch of the helical magnetic field lines in a tokamak, characterizes the magnetohydrodynamic (MHD) stability, confinement quality, and steadiness of the plasma. Note that the safety factor is a function of position and time since the magnetic field lines are not uniform and continuously evolve with time. The

variation of the safety factor from the magnetic axis to the plasma edge is referred to as the safety factor profile (refer to Figures 1). Studies have shown that MHD instabilities like the neoclassical tearing modes (NTMs) appear at locations where the safety factor is a rational number [1]. In particular, the lower order modes of NTMs corresponding to $q = 1.5$ and $q = 2$ are highly disruptive. By controlling the gradient of the safety factor profile at rational values of the safety factor, the effect of some MHD instabilities could be eliminated or at least mitigated.

The evolution of the safety factor profile is governed by a nonlinear partial differential equation (PDE) referred to as magnetic diffusion equation. Moreover, due to both the limited number of actuators and the limited control authority of each actuator, the controllability of the system is a key constraint during the control synthesis process. Active control of the safety factor profile has been an area of active research for more than one decade. The high dimensionality, nonlinearity, and limited controllability of the system, as well as the sensitivity of the control solution to each tokamak's specific characteristics (geometry, actuators, diagnostics, etc.) make the problem extremely difficult and rich. Most of the previous work in the field has focused either on minimizing the spatial integral of the squared tracking error or on controlling the safety factor values at fixed locations. The number of locations at which the safety factor can be independently controlled depends on the number of actuators available for control [2]. For instance, the algorithms proposed in [3], [4] control the safety factor value at just one location, namely, the magnetic axis (refer to Figure 1). On the other hand, controllers such as those developed in [2], [5] focus on controlling the safety factor values at a fixed number of pre-determined locations, while controllers such as those presented in [6], [7] focus on minimizing the squared error between actual and desired profiles integrated over the whole spatial domain. Different control techniques have been employed to address these problems based on a spatial discretization of the PDE model, including robust [7], [8], optimal [9], [6], and model predictive [10], [11] control. Alternatively, infinite-dimensional controllers (without spatially discretizing the dynamical model) have been developed in [12] under certain assumptions.

The common denominator of the previous work cited above is that the location where the safety factor is controlled is fixed in space. This is true regardless of whether one point, several points, or the spatial integral (over a fixed grid) of the profile are controlled. However, as mentioned before, the safety factor profile is continuously evolving over time. As

*This material is based upon work supported by the U.S. Department of Energy, Office of Science, Office of Fusion Energy Sciences, under Award Numbers DE-SC0010537 and DE-SC0010661. S. T. Paruchuri (saitejp@lehigh.edu) and E. Schuster are with the Department of Mechanical Engineering and Mechanics, Lehigh University, Bethlehem, PA 18015, USA. A. Pajares is with General Atomics, San Diego, CA 92121, USA.

a result, the locations of certain properties of the profile that may need to be controlled are also continuously changing with time. For instance, not only the value but also the location of the minimum of the safety factor profile change as the profile evolves. Moreover, the locations at which the safety factor profile achieves a particular value, for instance $q = 1.5$ or $q = 2$, continuously vary as the safety factor profile evolves over time. Modeling the dynamics of such profile properties for control design require nonautonomous differential equations, where the explicit time dependence arises from the time varying locations of these properties. Furthermore, controlling these properties as their spatial locations move can be inherently more challenging from a controllability perspective. This is because the location of the controlled profile property may drift to regions with lower actuation capability in certain scenarios. Control of spatially varying profile properties is a relatively new topic of research. Recent work in [13], [14] addresses the problem of controlling the spatial minimum of the safety factor profile. The problem of locally controlling the safety factor profile around a location associated with a specific rational value of the safety factor has not received much attention yet.

In this work, a control approach is proposed to regulate the gradient of the safety factor profile at the spatially moving location associated with a given rational value of the profile. The derivation of a model governing the evolution of the gradient of the safety factor profile is difficult, if not impossible. A bulk of the prior work cited above rely on a model for the gradient of the poloidal magnetic flux (formally defined in the following section), which is inversely related to the safety factor. Following a similar approach, a control model is proposed in this work for the evolution of the slope of the poloidal flux gradient. The target value for the safety factor gradient is translated into a target value for the slope of the poloidal flux gradient by using a central finite-difference approximation. Feedback linearization is later used to design a control algorithm to regulate the slope of the poloidal flux gradient at a location that evolves over time. Simulation results are presented to illustrate the capability of the designed controller to track a given constant slope target. The control-resolution presented in this work should be interpreted as a crucial initial step towards developing advanced local profile controllers that could eventually handle more complex targets as the actuation capability is increased (for instance, spatially moving actuators could enhance the controllers' capabilities). These advanced local controllers could play a critical role in keeping the system within MHD stability boundaries by shaping the profile at critical rational surfaces.

This paper is organized as follows. The control-oriented model derivation is introduced in Section II. In this model, the dynamics is governed by a nonautonomous ordinary differential equation. The controller synthesis is discussed in Section III. The results of numerical simulations performed to test the effectiveness of the controller are presented in Section IV. Finally, conclusions from this study and a discussion of potential future work are presented in Section V.

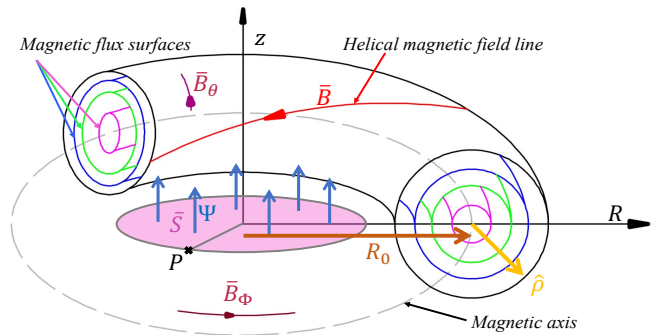


Fig. 1: Magnetic field lines inside a tokamak. The terms Ψ , \bar{B} , \bar{B}_θ , \bar{B}_ϕ and R_0 in the figure are the poloidal magnetic flux, total magnetic field, poloidal magnetic field, toroidal magnetic field and major radius of the tokamak, respectively.

II. CONTROL ORIENTED MODEL

A. Magnetic Diffusion Equation

The total magnetic field \bar{B} is composed by the poloidal magnetic field \bar{B}_θ and toroidal magnetic field \bar{B}_ϕ , respectively (see Figure 1). The poloidal magnetic flux at a point P in the tokamak is given by $\Psi := \int_{\bar{S}} \bar{B}_\theta \cdot d\bar{S}$. In this equation, the term \bar{S} denotes the surface perpendicular to the z direction and enclosed by the toroidal ring passing through the point P , as shown in Figure 1. The poloidal stream function ψ is defined as the poloidal magnetic flux per unit radian, that is, $\psi = \Psi/2\pi$. A magnetic flux surface is a region in the tokamak where the poloidal magnetic flux is constant. Under ideal MHD conditions, the magnetic flux surfaces are concentric, as shown in Figure 1. Magnetic flux surfaces are crucial since several plasma parameters like the safety factor q and the plasma pressure remain constant on any given surface under ideal MHD conditions. Combining this with the fact that tokamaks are toroidally axisymmetric by design, it is sufficient to consider one spatial dimension instead of three dimensions for the plasma evolution model used for control design. The normalized mean effective minor radius $\hat{\rho} \in [0, 1]$ is used in this work as the one-dimensional spatial variable indexing the nested magnetic flux surfaces. The mean effective minor radius ρ is defined as $\rho := \sqrt{B_{\phi,0}\pi/\Phi}$, where $B_{\phi,0}$ is the magnitude of the vacuum toroidal magnetic field at the major radius R_0 , and Φ is the toroidal magnetic flux. The normalized mean effective minor radius is defined as $\hat{\rho} := \rho/\rho_b$, where ρ_b is the mean effective minor radius at the last closed magnetic surface.

The magnetic diffusion equation (MDE) is used as the primary governing model for the evolution of the poloidal stream function ψ [15]. It is given by

$$\frac{\partial \psi}{\partial t} = \frac{\eta}{\mu_0 \rho_b^2 \hat{r}^2} \frac{1}{\hat{\rho}} \frac{\partial}{\partial \hat{\rho}} \left(\hat{\rho} D_\psi \frac{\partial \psi}{\partial \hat{\rho}} \right) + R_0 \hat{H} \eta j_{ni} \quad (1)$$

subject to the boundary conditions

$$\frac{\partial \psi}{\partial \hat{\rho}} \Big|_{\hat{\rho}=0} = 0, \quad \frac{\partial \psi}{\partial \hat{\rho}} \Big|_{\hat{\rho}=1} = - \underbrace{\frac{\mu_0 R_0}{2\pi \hat{G}_{\hat{\rho}=1} \hat{H}_{\hat{\rho}=1}}}_{k_{I_p}} I_p, \quad (2)$$

where η is the plasma resistivity, j_{ni} is the non-inductive current, μ_0 is the vacuum permeability, I_p is the plasma current, $\hat{F}, \hat{G}, \hat{H}$ are functions of $\hat{\rho}$ and are geometric factors pertaining to the magnetic configuration of a particular MHD equilibrium, and $D_\psi := \hat{F}\hat{G}\hat{H}$. The plasma resistivity η and the non-inductive current j_{ni} are modeled in this work using the relations developed in [16] with emphasis on control design. Readers can refer to the cited reference for a detailed explanation of the models and how they were generated. The control-oriented models for η and j_{ni} are given by

$$\eta \approx g_\eta \times (I_p^\gamma P_{tot}^\epsilon \bar{n}_e^\zeta)^{-3/2}, \quad (3)$$

$$\begin{aligned} \eta j_{ni} \approx & \sum_{i=1}^{N_{NBI}} g_{NBI,i} \times (I_p^\gamma P_{tot}^\epsilon \bar{n}_e^\zeta)^{(-3/2+\epsilon_{NBI})} \bar{n}_e^{-1} P_{NBI,i} \\ & + g_{EC} \times (I_p^\gamma P_{tot}^\epsilon \bar{n}_e^\zeta)^{(-3/2+\epsilon_{EC})} \bar{n}_e^{-1} P_{EC} \\ & + (\partial\psi/\partial\hat{\rho})^{-1} g_{BS} \times (I_p^\gamma P_{tot}^\epsilon \bar{n}_e^\zeta)^{-1/2} \bar{n}_e. \end{aligned} \quad (4)$$

In the above equations, the functions $g_\eta : \hat{\rho} \rightarrow g_\eta(\hat{\rho})$, $g_{BS} : \hat{\rho} \rightarrow g_{BS}(\hat{\rho})$ account for the spatial variation of the plasma resistivity and bootstrap current deposition. The term P_{tot} is the total injected power, \bar{n}_e is the line-average electron density, and γ, ϵ and ζ are scaling constants.

A neutral beam injector (NBI) injects a beam of high-energy neutral particles to drive current and heat the plasma. Alternatively, an electron cyclotron current drive (ECCD) projects electromagnetic waves whose frequency matches the electron cyclotron frequency. This results in electron cyclotron resonance which then heats the plasma and drives current. In this paper, it is assumed that there are N_{NBI} individual NBIs and 1 ECCD group available for control. In other words, the NBI powers $P_{NBI,i}$, for $i = 1, \dots, N_{NBI}$, and the ECCD power P_{EC} in (4) are the controllable inputs. This configuration aligns with the DIII-D tokamak configuration [17]. Nevertheless, the controller synthesized in the following section can be extended to other tokamaks also. In (4), the functions $g_{NBI,i} : \hat{\rho} \rightarrow g_{NBI,i}(\hat{\rho})$ and $g_{EC} : \hat{\rho} \rightarrow g_{EC}(\hat{\rho})$ represent the NBI and EC current deposition profiles, respectively. The terms $\epsilon_{NBI}, \epsilon_{EC}$ account for the efficiency of the NBI, EC actuators, respectively. The plasma current I_p , the line-average electron density \bar{n}_e and the total power P_{tot} are assumed to be regulated by other controllers around prescribed values. For instance, the plasma β (ratio of the plasma kinetic pressure to the magnetic pressure) controller prescribes the total power P_{tot} [2]. Note that the P_{tot} can also be expressed using the relation

$$P_{tot} = \sum_{i=1}^{N_{NBI}} P_{NBI,i} + P_{EC}. \quad (5)$$

Since $P_{NBI,i}, P_{EC}$ are controllable inputs and P_{tot} is a prescribed input, the controller must satisfy the above constraint at all times.

B. Safety Factor Profile

The safety factor profile $q : (\hat{\rho}, t) \mapsto q(\hat{\rho}, t)$ is defined using the relation

$$q(\hat{\rho}, t) := - (B_{\phi,0} \rho_b^2 \hat{\rho}) / \theta(\hat{\rho}, t), \quad (6)$$

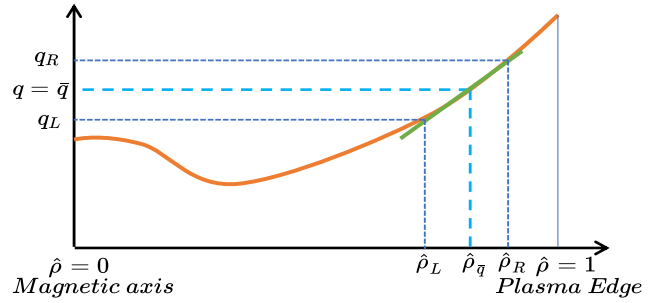


Fig. 2: q -profile gradient approximation at rational surface.

where $\theta := \frac{\partial\psi}{\partial\hat{\rho}}$ is the poloidal flux gradient. The terms $B_{\phi,0}$ and ρ_b are defined above. The goal of this paper is to control the q profile gradient q' at a pre-defined safety factor value. The notation $(\cdot)'$ represents the derivative with respect to the spatial variable $\hat{\rho}$. Suppose that the gradient has to be controlled at the location of the rational safety factor value $\bar{q} \in \mathbb{Q}^+$, where \mathbb{Q}^+ is the set of positive rational numbers. Let $\hat{\rho}_{\bar{q}} : t \mapsto \hat{\rho}_{\bar{q}}(t)$ represent the function that gives the $\hat{\rho}$ value at which the q profile attains \bar{q} at a given time t . That is, $q(\hat{\rho}_{\bar{q}}(t), t) = \bar{q}$. It is possible that the q profile achieves \bar{q} at multiple locations. In such cases, one of the multiple locations is selected a priori as the control point $\hat{\rho}_{\bar{q}}(t)$. In the following analysis, the notation (t) is dropped.

To simplify control design, the gradient of the q profile is approximated using a central finite difference scheme, i.e.

$$q'(\hat{\rho}_{\bar{q}}) \approx (q(\hat{\rho}_{\bar{q}} + h) - q(\hat{\rho}_{\bar{q}} - h)) / 2h, \quad (7)$$

where $h \in \mathbb{R}$. Since the term h is a constant, the gradient of the q profile can be controlled by controlling the difference $q(\hat{\rho}_{\bar{q}} + h) - q(\hat{\rho}_{\bar{q}} - h)$. In the following analysis, the terms $q(\hat{\rho}_{\bar{q}} + h)$, $q(\hat{\rho}_{\bar{q}} - h)$ are represented as q_R and q_L , respectively. Also, the locations of these points are represented using the notation $\hat{\rho}_R$ and $\hat{\rho}_L$, respectively. Note that the terms $q_R, q_L, \hat{\rho}_R$ and $\hat{\rho}_L$ are functions of time and can vary with the evolution of the q profile.

C. Plasma model for gradient control

Equation (6) shows us that the safety factor is related to the poloidal flux gradient θ . However, the MDE, given in (1), defines the plasma dynamics in terms of the poloidal stream function ψ . From a control design perspective, it is more convenient to work with a model that defines the evolution of $\theta(\hat{\rho}, t)$. To obtain such a model, (3) and (4) are substituted into (1) and the spatial derivative of the MDE is taken on both sides. This results in

$$\begin{aligned} \dot{\theta} = & (h_{\eta,1}\theta'' + h_{\eta,2}\theta' + h_{\eta,3}\theta) u_\eta + \sum_{i=1}^{N_{NBI}} h_{NBI,i} u_{NBI,i} \\ & + h_{EC} u_{EC} + \left(h_{BS,1} \frac{1}{\theta} - h_{BS,2} \frac{\theta'}{\theta^2} \right) u_{BS}, \end{aligned} \quad (8)$$

subject to the boundary conditions

$$\theta(0, t) = 0, \quad \theta(1, t) = -k_{I_p} I_p, \quad (9)$$

where

$$(\dot{\cdot}) := \frac{\partial}{\partial t}(\cdot), \quad (\cdot)' := \frac{\partial}{\partial \hat{\rho}}(\cdot), \quad h_{\eta,1} := \frac{1}{\mu_0 \rho_b^2} \frac{g_\eta}{\hat{F}^2} D_\psi,$$

$$\begin{aligned}
h_{\eta,2} &:= \frac{1}{\mu_0 \rho_b^2} \left[\left(\frac{g_\eta}{\hat{F}^2} \right)' D_\psi + \frac{g_\eta}{\hat{F}^2} \left(\frac{D_\psi}{\hat{\rho}} + 2D'_\psi \right) \right], \\
h_{\eta,3} &:= \frac{1}{\mu_0 \rho_b^2} \left[\left(\frac{g_\eta}{\hat{F}^2} \right)' \left(\frac{D_\psi}{\hat{\rho}} + D'_\psi \right) + \frac{g_\eta}{\hat{F}^2} \left(\frac{D'_\psi \hat{\rho} - D_\psi}{\hat{\rho}^2} \right) \right], \\
h_{NBI,i} &:= R_0 \times (\hat{H} \times g_{NBI,i})', \quad h_{EC} := R_0 \times (\hat{H} \times g_{EC})', \\
h_{BS,1} &:= R_0 \times (\hat{H} \times g_{BS})', \quad h_{BS,2} := R_0 \times \hat{H} \times g_{BS}, \\
u_\eta &:= (I_p^\gamma P_{tot}^\epsilon \bar{n}_e^\zeta)^{-3/2}, \quad u_{BS} := (I_p^\gamma P_{tot}^\epsilon \bar{n}_e^\zeta)^{-1/2} \bar{n}_e, \\
u_{NBI,i} &:= (I_p^\gamma P_{tot}^\epsilon \bar{n}_e^\zeta)^{(-3/2 + \zeta_{NBI})} \bar{n}_e^{-1} P_{NBI,i}, \\
u_{EC} &:= (I_p^\gamma P_{tot}^\epsilon \bar{n}_e^\zeta)^{(-3/2 + \zeta_{EC})} \bar{n}_e^{-1} P_{EC}.
\end{aligned} \tag{10}$$

The detailed steps involved in the derivation of the above equation are given in [2]. In the above equations, the terms $h_{\eta,1}, h_{\eta,2}, h_{\eta,3}, h_{NBI,i}, h_{EC}, h_{BS,1}$ and $h_{BS,2}$ are functions of the spatial variable $\hat{\rho}$. Alternatively, the terms $u_\eta, u_{NBI,i}, u_{EC}$ and u_{BS} are functions of time and can be considered as virtual inputs.

The above PDE defines the evolution of the whole θ profile. However, it is sufficient to consider the dynamics at $\hat{\rho}_L$ and $\hat{\rho}_R$. To simplify the PDE, define $\theta_L = \theta(\hat{\rho}_L(\cdot), \cdot)$, $\theta'_L = \theta'(\hat{\rho}_L(\cdot), \cdot)$, $\theta''_L = \theta''(\hat{\rho}_L(\cdot), \cdot)$, $h^L_{(\cdot)} = h_{(\cdot)} \circ \hat{\rho}_L$. Define the terms $\theta_R, \theta'_R, \theta''_R$ and $h^R_{(\cdot)}$ similarly. After evaluating the spatial term at $\hat{\rho}_L$ and $\hat{\rho}_R$, the autonomous partial differential equation considered above simplifies into two coupled non-autonomous ordinary differential equations of the form

$$\dot{\theta}_L = \hat{h}_L^T \hat{u} + \hat{c}_L, \quad \dot{\theta}_R = \hat{h}_R^T \hat{u} + \hat{c}_R, \tag{11}$$

where, for $i \in \{L, R\}$,

$$\begin{aligned}
\hat{h}_i &= [h^i_{NBI,1}, \dots, h^i_{NBI, N_{NBI}}, h^i_{EC}]^T, \\
\hat{u} &= [u_{NBI,1}, \dots, u_{NBI, N_{NBI}}, u_{EC}]^T, \\
\hat{c}_i &= (h^i_{\eta,1} \theta''_i + h^i_{\eta,2} \theta'_i + h^i_{\eta,3} \theta_i) u_\eta + \left(h^i_{BS,1} \frac{1}{\theta_i} - h^i_{BS,2} \frac{\theta'_i}{\theta_i^2} \right) u_{BS}.
\end{aligned}$$

Now, define the difference θ_D of the poloidal flux gradients at $\hat{\rho}_R$ and $\hat{\rho}_L$ as $\theta_D := \theta_R - \theta_L$. Thus, the evolution of the difference in poloidal flux gradients θ_D is given by

$$\dot{\theta}_D = \dot{\theta}_R - \dot{\theta}_L. \tag{12}$$

Before proceeding to the controller synthesis, note that the goal of the controller is to track a target safety factor gradient \bar{q}' where the safety factor profile achieves a value of \bar{q} . However, the control-oriented model is defined in terms of the poloidal flux gradient difference θ_D . Thus, it is important to reformulate the target in terms of the poloidal flux gradient difference. In the following analysis, it is assumed that the location $\hat{\rho}_{\bar{q}}$ at which the safety factor profile achieves the value \bar{q} is known at all time t . During tokamak operation, real-time equilibrium reconstruction techniques are used to determine the safety factor profile [18]. Thus, at any given time instant, it is possible to determine the point $\hat{\rho}_{\bar{q}}$ at which the profile is equal to the rational value \bar{q} . The first step in redefining the target in terms of θ_D involves approximating the target gradient \bar{q}' using the central difference scheme as

$$\bar{q}' \approx (\bar{q}_R - \bar{q}_L) / 2h, \tag{13}$$

where $\bar{q}_R := \bar{q}(\hat{\rho}_R)$, $\bar{q}_L := \bar{q}(\hat{\rho}_L)$, and the term $h \in \mathbb{R}$ is the constant used in (7). Since h is fixed a priori and $\hat{\rho}_{\bar{q}}$ is known

at each time instant, the location of the two control points $\hat{\rho}_R$ and $\hat{\rho}_L$ can be determined using the relations $\hat{\rho}_R := \hat{\rho}_{\bar{q}} + h$ and $\hat{\rho}_L := \hat{\rho}_{\bar{q}} - h$. Even if the target profile \bar{q} is not prescribed, the values \bar{q}_R and \bar{q}_L can be determined using the assumption that the target safety factor profile is such that a straight line connects \bar{q}_R and \bar{q}_L at $\hat{\rho}_R$ and $\hat{\rho}_L$, respectively. This assumption is inherent in the central difference scheme used to approximate the gradient. Figure 2 demonstrates the assumption for a generate safety factor profile q . Now, the redefined target $\bar{\theta}_D$ can be computed using the relation $\bar{\theta}_D = \bar{\theta}_R - \bar{\theta}_L$, where $\bar{\theta}_L$ and $\bar{\theta}_R$ are given by the equation

$$\bar{\theta}_i(t) = - (B_{\phi,0} \rho_b^2 \hat{\rho}_i(t)) / \bar{q}_i(t), \quad \text{for } i \in \{L, R\}. \tag{14}$$

As the closed loop system evolves, the location $\hat{\rho}$ at which the rational safety factor value \bar{q} is achieved varies with time. This in turn implies that the terms $\hat{\rho}_L$ and $\hat{\rho}_R$ also vary with time. Thus, strictly speaking, the target θ_D is a function of time t even if a constant safety factor gradient target \bar{q}' is initially chosen. In certain operation scenarios, the change in $\hat{\rho}_L$ and $\hat{\rho}_R$ over time is minimal. In such cases, a constant \bar{q}' can be reformulated as a fixed target $\bar{\theta}_D$.

III. CONTROLLER DESIGN

A. Feedback Linearization

In this work, feedback linearization is used to first linearize the system and then design a controller with proportional and integral action. Since the controller can only influence the actuator power values $u = [P_{NBI,1}, \dots, P_{NBI, N_{NBI}}, P_{EC}]$, define h_L and h_R such that $\hat{h}_L^T \hat{u} = h_L^T u$ and $\hat{h}_R^T \hat{u} = h_R^T u$ hold. Also, assume that there is a feedforward component in the inputs. That is, $u = u_{ff} + u_{fb}$, where u_{ff} and u_{fb} are the feedforward and the feedback components, respectively. With the introduction of the new definitions, the governing equations take the form

$$\dot{\theta}_D = h_D^T u_{fb} + \check{c}_D, \tag{15}$$

where $u_k = [P_{NBI,k,1}, \dots, P_{NBI,k, N_{NBI}}, P_{EC,k}]^T$ for $k = ff, fb$, $\check{c}_D = \check{c}_R - \check{c}_L$, $\check{c}_i = \hat{c}_i + h_i^T u_{ff}$ for $i = L, R$, $h_D = h_R - h_L$. Define the state error $\tilde{\theta}_D$ as $\theta_D := \theta_D - \bar{\theta}_D$, where $\bar{\theta}_D$ is the target. To feedback linearize the system, the inputs u_{fb} are chosen such the equation

$$\dot{\tilde{\theta}}_D = -K_p \tilde{\theta}_D - K_I \int_0^t \tilde{\theta}_D dt \tag{16}$$

holds for all time t . This is equivalent to

$$h_D^T u_{fb} + c_D = 0, \tag{17}$$

where $c_D = \check{c}_D + K_p \bar{\theta}_D + K_I \int_0^t \bar{\theta}_D dt$. To analyze the stability of (16), define $x := [\tilde{\theta}_D, \int_0^t \tilde{\theta}_D d\tau]^T$ and consider the Lyapunov function V given by $V = \frac{1}{2} x^T \begin{bmatrix} 1 & b \\ b & K_I \end{bmatrix} x$. Here, the constant b is assumed to satisfy the inequality $0 < b < \min(\sqrt{K_I}, K_p, K_p K_I / (K_I + \frac{1}{4} K_p^2))$. Taking the derivative of V with respect to time t results in the equation

$$\dot{V} = -(K_p - b) \tilde{\theta}_D^2 - K_I b \left(\int_0^t \tilde{\theta}_D d\tau \right) - K_p b \tilde{\theta}_D \int_0^t \tilde{\theta}_D d\tau,$$

which is negative definite. Thus, using Lyapunov theorem [19], we conclude that the origin is asymptotically stable. In the presence of uncertainties, the state trajectory can be shown to converge to a neighborhood of the origin.

B. Optimization

Since there are $N_{NBI} + 1$ actuators and 2 equality constraints (5) and (17), infinite combinations of the input values may achieve the required feedback linearization at a given time instant. To select a unique set of optimal feedback inputs, an optimization problem is solved at each time t . The goal of the optimization problem is to minimize the feedback “control effort” f defined as

$$f(u_{fb}) = u_{fb}^T Q u_{fb}, \quad (18)$$

with respect to the feedback input power u_{fb} subject to the constraints

$$\begin{bmatrix} h_D^T & & \\ 1 & \cdots & 1 \end{bmatrix} u_{fb} = \begin{bmatrix} -c_D \\ P_{tot,fb} \end{bmatrix}, \quad (19)$$

and the actuator saturation limits at each time t . Note that the term $P_{tot,fb}$ is defined as $P_{tot,fb} = P_{tot} - \left(\sum_{i=1}^{N_{NBI}} P_{NBI,ff,i} + P_{EC,ff} \right)$ and Q is a symmetric positive definite matrix. Ignoring the actuator saturation limits, the above optimization problem has a closed-form solution. To derive this, define the constraint functions g_1 , and g_2 as

$$g_1(u_{fb}) = h_D^T u_{fb} + c_D, \quad g_2(u_{fb}) = \mathbb{1}^T u_{fb} + c_p, \quad (20)$$

where $c_p = -P_{tot,fb}$, and $\mathbb{1} = [1, \dots, 1]^T \in \mathbb{R}^{N_{NBI}+1}$. Now, the Lagrangian can be defined as

$$\mathcal{L}(u_{fb}, \lambda_1, \lambda_2) = f(u_{fb}) - \lambda_1 g_1(u_{fb}) - \lambda_2 g_2(u_{fb}). \quad (21)$$

Lagrange multipliers theorem states that if u_{fb}^* is an extremum, then there exist λ_1^* and λ_2^* such that the condition $\nabla \mathcal{L}(u_{fb}^*, \lambda_1^*, \lambda_2^*) = 0$ holds. Solving this equation gives an expression for inputs u_{fb}^* of the form

$$u_{fb}^* = \frac{1}{2} Q^{-1} \begin{bmatrix} h_D & \mathbb{1} \end{bmatrix} \mathbb{A}^{-1} \mathbf{c}, \quad (22)$$

where

$$\mathbb{A} = \begin{bmatrix} h_D^T Q^{-1} h_D & h_D^T Q^{-1} \mathbb{1} \\ \mathbb{1}^T Q^{-1} h_D & \mathbb{1}^T Q^{-1} \mathbb{1} \end{bmatrix}, \quad \mathbf{c} = \begin{bmatrix} -2c_D \\ -2c_p \end{bmatrix}. \quad (23)$$

Incorporating actuator constraints introduces inequality constraints into the optimization problem. Readers can refer to the iterative algorithm introduced in [14] to calculate the optimal solution with the actuator constraints satisfied.

IV. NUMERICAL VALIDATION OF CONTROLLER

This section discusses the results of simulations carried out using the Control Oriented Transport SIMulator (COT-SIM), which uses the 1D magnetic diffusion equation (1)-(2) in combination with a heat transport equation based on the Bohm/Gyro-Bohm transport model for simulating the tokamak plasma dynamics [20]. The simulations used the configuration of the DIII-D tokamak, and the inputs from DIII-D shot 147634. The feedforward input u_{ff} was selected

as $u_{ff} = 0.9u_{147634}$, where u_{147634} is the corresponding vector of actuator powers used in DIII-D shot 147634. During a typical DIII-D discharge of around 6 seconds, the spatial location associated with a given rational safety factor value (for example, $\hat{\rho}_{\bar{q}}$ corresponding to $\bar{q} = 1.5$) can vary significantly. In this case, there is a possibility for $\hat{\rho}_{\bar{q}}$ to move to locations with lower actuator authority (regions corresponding to low noninductive current depositions). In order to decouple the assessment of the controller’s performance from a varying actuator authority, the simulation study was carried out in this case by extending the length of the discharge (beyond DIII-D’s practical limits) and by activating the controller once the temporal evolution of the safety factor profile is negligible. Linear extrapolation was used in this simulation study to generate the feedforward input data beyond 6 seconds. The cost function matrix Q used in the simulation was selected as $Q = \text{diag}(1,1,1)$, implying that all the noninductive current drives are given equal importance. Furthermore, the controller gains were selected as $K_P = 5 \times 10^{-3}$ and $K_I = 1 \times 10^{-4}$. The actuator powers $P_{NBI,1}$, $P_{NBI,2}$ and P_{EC} were allowed to take values in the closed intervals $[0, 12]$, $[0, 6]$ and $[0, 3.5]$, respectively.

Figure 3 denotes the evolution of θ_D in the feedforward-only and the feedforward+feedback cases. Since the safety factor profile variation is negligible once the controller is activated, the term θ_D remains constant in the feedforward-only case. It is clear from the figure that the closed-loop system achieves the desired target within 5 seconds. Figure 3 also shows where the q profile achieves its minimum and the target $\bar{q} = 1.5$, denoted by $\hat{\rho}_{q_{min}}$ and $\hat{\rho}_{\bar{q}}$, respectively. Since $\hat{\rho}_{\bar{q}}$ is away from $\hat{\rho}_{q_{min}}$, the central difference scheme given in (7) is a reasonably good approximation for the safety factor profile gradient for $h = 0.1$. The left and right control points, denoted by $\hat{\rho}_L$ and $\hat{\rho}_R$, respectively, are also shown in the figure. It is clear that $\hat{\rho}_{q_{min}}$, $\hat{\rho}_L$ and $\hat{\rho}_R$ vary (although minimally in this case) once the controller is activated. Figure 4 shows the open-loop (feedforward only) and the closed-loop (feedforward + feedback) simulation inputs. The grey background in Figures 3 and 4 denote the time when the controller is active.

V. CONCLUSION AND FUTURE WORK

A model-based nonlinear control algorithm has been proposed for the first time to locally regulate the gradient of the safety-factor profile at the location of a given rational safety-factor value in tokamak plasmas. The model used for control synthesis accounts for the inherent variation over time of the spatial location associated with the rational safety factor value of interest. A controller based on the feedback linearization of this model has been synthesized to regulate the gradient of the safety factor profile around a desired value. Closed-loop simulations based on the COTSIM code shows that the proposed controller can track selected targets in DIII-D scenarios. The simulations in this work assume constant targets, which simplifies the controller implementation and facilitates the development of an initial understanding of

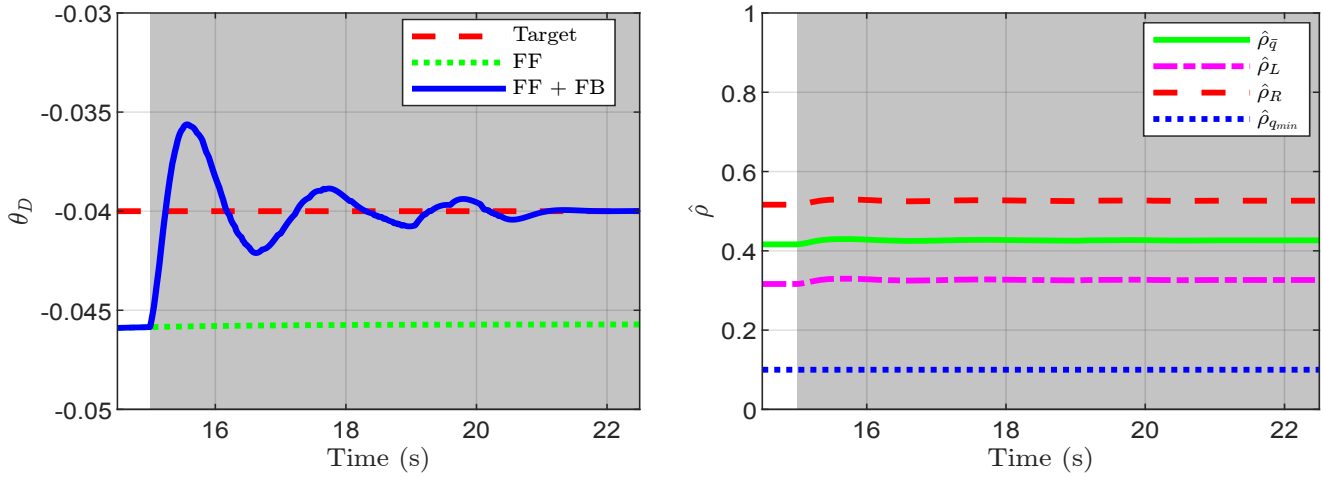


Fig. 3: Poloidal flux gradient difference θ_D (left), Target spatial points (right).

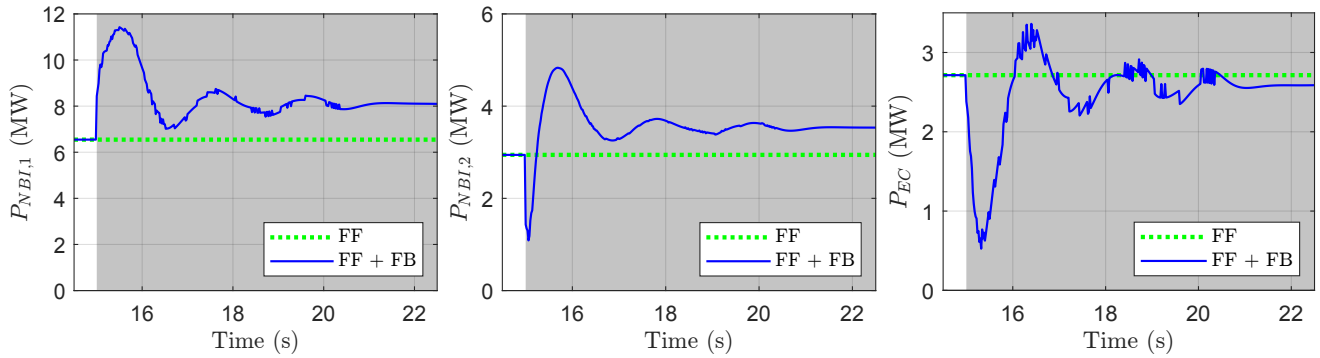


Fig. 4: Auxiliary powers - $P_{NBI,1}$ (left), $P_{NBI,2}$ (center), P_{EC} (right)

the controller's capabilities. Future extensions of this work may focus on considering time-varying targets, using moving ECCD sources as spatially varying actuators, and integrating an optimal reference governor in order to keep the plasma operating point within MHD stability boundaries.

REFERENCES

- [1] J. Wesson and D. J. Campbell, *Tokamaks*. Oxford university press, 2011, vol. 149.
- [2] A. Pajares and E. Schuster, "Current profile and normalized beta control via feedback linearization and Lyapunov techniques," *Nucl. Fusion*, p. 21, 2021.
- [3] M. Boyer *et al.*, "Central safety factor and β_n control on NSTX-U via beam power and plasma boundary shape modification, using TRANSP for closed loop simulations," *Nuclear Fusion*, vol. 55, no. 5, p. 053033, Apr. 2015.
- [4] A. Pajares and E. Schuster, "Central safety factor control in DIII-D using neutral beam injection and electron cyclotron launchers in zero input-torque scenarios," in *2017 IEEE Conference on Control Technology and Applications (CCTA)*, Aug. 2017, pp. 1460–1465.
- [5] N. T. Vu *et al.*, "Plasma internal profile control using IDA-PBC: Application to TCV," *Fusion Engineering and Design*, vol. 123, pp. 624–627, Nov. 2017.
- [6] M. D. Boyer *et al.*, "First-principles-driven model-based current profile control for the DIII-D tokamak via LQI optimal control," *Plasma Physics and Controlled Fusion*, vol. 55, no. 10, p. 105007, Sep. 2013.
- [7] J. E. Barton *et al.*, "Physics-based control-oriented modeling and robust feedback control of the plasma safety factor profile and stored energy dynamics in ITER," *Plasma Physics and Controlled Fusion*, vol. 57, no. 11, p. 115003, Sep. 2015.
- [8] W. Wehner *et al.*, "Optimal current profile control for enhanced repeatability of L-mode and H-mode discharges in DIII-D," *Fusion Engineering and Design*, vol. 123, pp. 513–517, Nov. 2017.
- [9] C. Xu *et al.*, "Sequential linear quadratic control of bilinear parabolic PDEs based on POD model reduction," *Automatica*, vol. 47, no. 2, pp. 418–426, Feb. 2011.
- [10] Y. Ou *et al.*, "Receding-horizon optimal control of the current profile evolution during the ramp-up phase of a tokamak discharge," *Control Engineering Practice*, vol. 19, no. 1, pp. 22–31, Jan. 2011.
- [11] E. Maljaars *et al.*, "Profile control simulations and experiments on TCV: A controller test environment and results using a model-based predictive controller," *Nuclear Fusion*, vol. 57, no. 12, p. 126063, Oct. 2017.
- [12] F. B. Argomedeo *et al.*, "Lyapunov-based distributed control of the safety-factor profile in a tokamak plasma," *Nuclear Fusion*, vol. 53, no. 3, p. 033005, Feb. 2013.
- [13] A. Pajares and E. Schuster, "Robust Nonlinear Control of the Minimum Safety Factor in Tokamaks," in *5th IEEE Conference on Control Technology and Applications*, 2021.
- [14] S. T. Paruchuri *et al.*, "Minimum safety factor control in tokamaks via optimal allocation of spatially moving electron cyclotron current drive," in *60th IEEE Conference on Decision and Control*, 2021.
- [15] F. L. Hinton and R. D. Hazeltine, "Theory of plasma transport in toroidal confinement systems," *Reviews of Modern Physics*, vol. 48, no. 2, pp. 239–308, Apr. 1976.
- [16] J. E. Barton *et al.*, "Physics-based control-oriented modeling of the safety factor profile dynamics in high performance tokamak plasmas," in *52nd IEEE Conference on Decision and Control*, Dec. 2013, pp. 4182–4187.
- [17] "DIII-D National Fusion Facility," <https://www.ga.com/magnetic-fusion/diii-d>.
- [18] J. Ferron *et al.*, "Real time equilibrium reconstruction for tokamak discharge control," *Nuclear Fusion*, vol. 38, no. 7, pp. 1055–1066, jul 1998.
- [19] H. K. Khalil, *Nonlinear Systems*, 3rd ed. Pearson, 2002.
- [20] A. Pajares, "Integrated Control in Tokamaks using Nonlinear Robust Techniques and Actuator Sharing Strategies," Ph.D. dissertation, Lehigh University, Bethlehem, PA, USA, 2019.